Inhibiting aberrant Stat3 function with molecular therapeutics: a progress report

Sina Haftchenary, Miriam Avadisian and Patrick T. Gunning

Aberrantly activated signal transducer and activator of transcription 3 (Stat3) protein plays a master regulatory role in the progression and survival of human cancers through the upregulation of target protooncogenes. Numerous human cancers, including breast, ovarian, prostate, leukemia, lymphoma, multiple myeloma, and brain cancers have been shown to harbor constitutively active Stat3 protein resulting in the expression of protooncogenes. The transcriptionally active Stat3–Stat3 protein homodimer has been extensively targeted as a means to suppress the aberrant Stat3 function in human cancer. This review will outline the recent progress made toward identifying drug-like compounds capable of effectively inhibiting aberrant Stat3 signaling through the disruption of Stat3 protein–protein interactions.
***Anti-Cancer Drugs* 22:115–127 © 2011 Wolters Kluwer Health | Lippincott Williams & Wilkins.**

Anti-Cancer Drugs 2011, **22**:115–127

Keywords: anticancer drugs, molecular recognition, protein–protein interactions, small molecule inhibitors, Stat3

Department of Chemistry, University of Toronto, Mississauga, Canada

Correspondence to Professor Patrick T. Gunning, PhD, Department of Chemistry, University of Toronto, 3359 Mississauga Rd. North, South Building, Rm4046, Mississauga, ON L5L 1C6, Canada
Tel: +1 905 569 4588; fax: +1 905 828 5425;
e-mail: patrick.gunning@utoronto.ca

Sina Haftchenary and Miriam Avadisian contributed equally to this work

Received 26 August 2010 **Revised form accepted** 1 October 2010

Introduction

Signal transducers and activators of transcription (STAT) proteins are a family of cytosolic transcription factors that mediate the downstream signaling of activated cytokine and growth factor receptors. STAT proteins play an important role in regulating the expression of specific target genes that promote cell growth, survival, differentiation, development, and inflammation [1–3]. Thus, the STATs play a dual role, both in signal transduction and gene transcription, in which they facilitate the relay of extracellular signals from membrane-associated receptors to the nucleus and promote expression of target genes [4,5]. The mammalian STAT family has seven members (Stat1, Stat2, Stat3, Stat4, Stat5α, Stat5β, and Stat6), each encoded by different genes [3]. Structurally, the STAT family has six conserved domains that include the N-terminal domain [6], coiled-coil domain [7], DNA binding domain [8], linker domain, Src-homology 2 (SH2) domain [8], and a C-terminal transactivation domain [9].

Cytokine or growth factor-induced activation of the Stat3 isoform results in the upregulation of Stat3 target protooncogenes that control cellular proliferation, differentiation, and survival. In contrast to normal cells, in which Stat3 activation is rapid and transient, cancer cells routinely harbor constitutively activated Stat3 proteins that promote a permanent alteration of genes that control fundamental cellular processes. Persistent activation of Stat3 promotes tumorigenesis and cancer progression through the upregulation of cell-survival proteins (Bcl-x_L, Bcl-2) [10,11], and cell cycle regulators (c-Myc, cyclin D1/D2) [12], and by the induction of angiogenesis [13]. Numerous studies have shown that Stat3 plays an aberrant role in ovarian [14,15], breast [15], prostate [16], leukemia [17], lymphoma [18], and head and neck [19] cancer cells, and that downregulation of this oncogene through iRNA knockdown induces cellular apoptosis (Fig. 1).

The canonical view of Stat3 signaling describes latent Stat3 protein (in an inactive monomeric/dimeric form) as residing predominantly in the cytoplasm. Ligand binding to the extracellular domain of transmembrane receptors induces intracellular activation of tyrosine kinases, such as Janus kinases (JAKs). Receptors are phosphorylated on critical Tyr residues, creating docking sites for the recruitment of unphosphorylated Stat3 protein through its SH2 domain. Stat3 is phosphorylated on a key Tyr residue (Tyr705), which leads to receptor dissociation and the formation of activated Stat3–Stat3 dimers through reciprocal SH2–pTyr705 interactions [20,21]. After translocation to the nucleus, dimeric Stat3 complexes bind to DNA response elements and promote gene transcription [22].

As a critical step in Stat3 homodimerization, the Stat3 SH2 domain engages the pTyr705-containing segment of the cognate phosphopeptide through a trigonal arrangement of binding subdomains. Specifically, the binding surface contains (i) a hydrophilic cleft formed by Arg609, Ser611, Glu612, Ser613, and Lys591; (ii) a predominantly hydrophobic pocket formed by Ile597, Ile634, and the tetramethylene portion of Lys592 and the Arg595 side chain; and (iii) a hydrophobic groove consisting of Phe716 and Trp623 [21]. As a result of its functional significance, the majority of anti-Stat3 research has focused on mimicking the Stat3 phosphopeptide binding sequence

0959-4973 © 2011 Wolters Kluwer Health | Lippincott Williams & Wilkins DOI: 10.1097/CAD.0b013e328341185b

Fig. 1

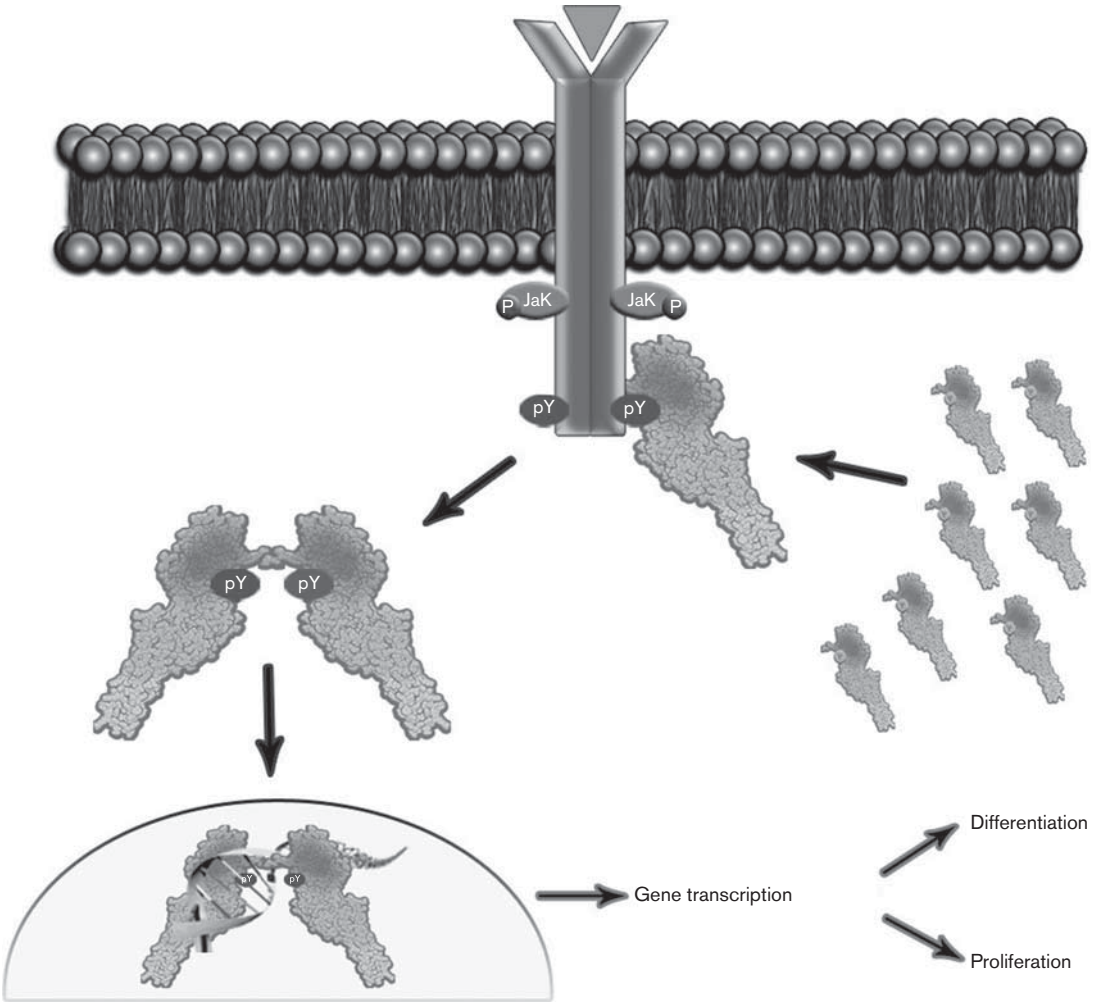

The JAK/Stat3 signaling pathway. Cytosolic Stat3 is recruited to membrane-associated JAK kinases and undergoes tyrosine phosphorylation (Tyr705). On dissociation, two phosphorylated Stat3 monomers homodimerize to form an active transcriptional complex. The dimer translocates to the nucleus in which it binds to the promoter regions on DNA to induce the transcription of protooncogenes responsible for cell growth, differentiation, and proliferation. Jak, Janus kinase; pY, phosphotyrosine.

to suppress the dimerization event. Notable alternative therapeutic strategies, including targeting Stat3's DNA binding site, N-terminal domain inhibitors, and SH2 domain mimicry, have also come to the forefront in recent years and will be discussed in this review. This review will cover Stat3 inhibitors found to directly bind Stat3, with particular emphasis given to inhibitors discovered in the last 5 years. Inclusion of upstream inhibitors of Stat3 is beyond the scope of this review.

Peptide and peptidomimetic inhibitors

Inhibiting Stat3 dimerization through peptidic inhibitors was first achieved by Turkson *et al.* [22], who used a truncated segment of the Stat3 native sequence (pYLKTK) to bind Stat3's SH2 domain and effectively compete with a phosphorylated Stat3 monomer (DB_{50} = 235 μmol/l). Similarly, Ren *et al.* [23] used a 7-mer phosphopeptide fragment of the gp130 receptor [Ac-pYLPQTV-NH_2 (Fig. 2-**1**)], a known Stat3 receptor, to potently bind the Stat3 SH2 domain and inhibit native phosphopeptide binding. In both cases, the peptide sequences exhibited poor cellular efficacy, requiring high doses to elicit a biological response. More recently, Diurlat *et al.* [24] identified a nonendogenous phosphopeptide, AYRNRpYRRQYRY, which displayed high affinity toward Stat3 *in vitro* (DB_{50} = 9.2 μmol/l). To test for cellular activity, Diurlat *et al.* coupled the peptide to an antennapedia cell-penetrating peptide sequence to afford an impressive DB_{50} of 9.7 μmol/l in NIH3T3/vSrc cells. As a control, the corresponding nonphosphorylated sequence was assessed for binding affinity and cellular activity in an enzyme-linked immunosorbent assay (ELISA). The nonphosphorylated peptide showed only weak activity (DB_{50} > 1 mmol/l). However, when coupled with antennapedia and subjected to

Fig. 2

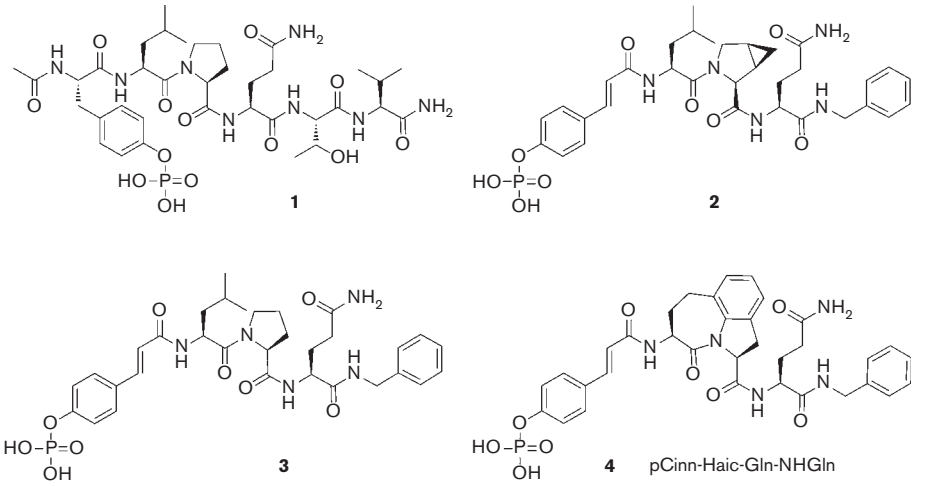

Chemical structures of peptidomimetics **1–4**.

NIH3T3/vSrc cells, the nonphosphorylated peptide showed enhanced activity (DB_{50} = 7.1 μmol/l). The antennapedia translocation sequence elicited only weak Stat3 inhibitory activity in isolation (DB_{50} = 291 μmol/l). Fluorescence microscopy experiments with fluorescein-labeled antennapedia peptide sequences and Texas Red-labeled Stat3 were used to visualize the effects on Stat3 localization and Stat3 colocalization with the peptides in NIH3T3/vSrc fibroblasts. Encouragingly, after incubation with either phosphorylated-antennapedia or nonphosphorylated-antennapedia sequences (50 μmol/l, 15 min) it was shown that predominantly nuclear residing Stat3 was significantly delocalized, resulting in a limited Stat3 nuclear presence and increased perinuclear and cytoplasmic membrane localizations. The antiproliferative activity of both these promising peptides was then evaluated and was shown to inhibit cell growth in a similar dose-dependent manner (IC_{50}–50 μmol/l).

Peptide inhibitors have served to inspire numerous innovative peptidomimetic analogs with reduced peptidic character, greater metabolic stability, increased structural rigidity, and enhanced drug-like characteristics. As an excellent example of peptidomimicry, Coleman *et al.* [25] have rationally reduced the peptidic character of the high-affinity peptide, Ac-pYLPQTV-NH_2 (**1**) (IC_{50} = 150 nmol/l), to furnish pCinn-Leu-*cis*-3,4-methanoPro-Gln-NHBn (Fig. 2-2), which, despite reduced peptidic character, retained excellent in-vitro binding activity (IC_{50} = 69 nmol/l). However, the researchers cited the expense of the *cis*-3,4-methanoproline as being prohibitive to further investigation, and thus considered the proline-containing peptidomimetic **3** (IC_{50} = 138 nmol/l), discovered in this same study, to be a more suitable candidate for further optimization (Fig. 2). In this study, Coleman *et al.* [25] and Mandal *et al.* [26] used a variety of phosphotyrosine mimetics including 4-phosphorylozycinnamate (pCinn), 5-phosphoryloxyindole-2-carboxylate (pInd), and 2-phosphoryloxy-7-carbonyl-naphthyl. The researchers showed that the conformationally constrained pCinn analog exhibited the highest affinity, and suggested that the constrained C-Cα-Cβ-Cγ dihedral angle positioned the phosphate group to optimally bind the protein.

In a separate study, Mandal *et al.* [27,28] reduced the peptidic character and susceptibility of **1** to cytosolic glutaminases and proteases by synthesizing a variety of glutamine mimetics including *O*-carbamoylserine, *O*-carbamoylthreonine, sulfonamide, 4-aminobutyric acid and constrained 4-aminobutyric acid analogs. However, the modified analogs were shown to have reduced binding affinity. The researchers concluded that the native unconstrained carboxamide side chain at the pY + 3 recognition site was necessary for the high-affinity SH2-binding affinity. In-silico docking studies showed the glutamine residue occupying a tight pocket on the protein surface with the side-chain carboxamide group participating in several hydrogen bonds [29].

Conformational constraints were incorporated in other locations of the SH2-binding peptide (**1**) in hopes that restricting backbone flexibility would decrease the entropic penalty of binding and enhance peptidomimetic affinity. Mandal *et al.* [26] replaced both the leucine and proline residues in **3** with a series of constrained cyclic units. Most notably, the researchers incorporated a tricyclic Haic {5-[(*S*)-amino]-1,2,4,5,6,7-hexahydroazepino (3,2,1–h*i*)indole-4-one-2-(*S*) carboxylate} unit to furnish the constrained inhibitor, pCinn-Haic-Gln-NHGln (Fig. 2, structure **4**). By fluorescence polarization (FP) assay, **4** was determined to have an impressive IC_{50} value of 162 nmol/l, a two-fold enhancement compared with hexapeptide **1**.

The importance of the pY + 3 Gln residue was illustrated with a series of analogs in which the Gln residue was deleted (pCinn-Haic-NH_2, IC_{50} = 35 600 nmol/l) or replaced (pCinn-Haic-Ala-NH_2, IC_{50} = 25 060 nmol/l), resulting in significant decreases in binding affinity. Although the reduced peptidic character of **4** should enhance whole-cell anti-Stat3 activity, both in terms of cell permeability and metabolic stability, at 25 μmol/l concentrations of **4** in MDA-MB-468 cells, the researchers reported negligible inhibition of phosphorylated Stat3 levels [30]. This was attributed to inhibitor inactivation by intracellular phosphatases.

Historically, phosphopeptide mimetics targeting SH2 domains have major drawbacks because of the polarity and lability of the phosphate ester moiety. In an attempt to improve the pharmacokinetic profile of phosphopeptidomimetics, Mandal *et al.* [30] adopted a phosphate ester prodrug strategy to improve the cellular activity of peptidomimetics **3** and **4** (Fig. 2). Moreover, reasoning that the phosphate ester group would be rapidly hyrolyzed *in vitro*, the researchers replaced it with an unhydrolyzable phosphonodifuoromethyl group. To mask the polarity of the phosphonate group, they protected the hydroxyl groups with pivaloyloxymethyl-protecting groups to afford analogs **5** and **6** (Fig. 3). To assess whole-cell activity, MDA-MB-468 breast tumor cells were subjected to these agents and assessed for inhibition of Stat3 phosphorylation levels. The least peptidic prodrug **6** (Fig. 3, analog of pCinn-Haic-Gln-NHBn), most potently inhibited Stat3 phosphorylation at concentrations of 10 μmol/l, compared with **5,** which required a five-fold increase in inhibitor concentration to elicit the same biological effect. Encouragingly, these results suggested that the prodrug strategy facilitated greater cell permeability of the peptidomimetic and furthermore, that cytoplasmic carboxy-esterases successfully cleave the pivaloyloxymethyl-protecting groups and show the active difluoromethylphosphonate group.

In a similar study, Dourlat *et al.* [31] replaced the pTyr of peptide **1** (IC_{50} = 9 μmol/l, as assessed by ELISA) with one of either a L-4-[(tetrazol-5-yl)methyl]phenylalanine, L-(*O*-malonyl) tyrosine, L-4-(phosphonomethyl)-phenylalanine, or a L-4-(tetrazol-5-yl)-phenylalanine group and assessed Stat3 dimerization disruption. The synthetic peptides were incubated with NIH3T3/vSrc nuclear extracts for 30 min at room temperature before incubation in an ELISA plate, precoated with Stat3 binding oligonucleotides. The results showed that **7**, possessing the dianionic malonic acid group, exhibited moderate activity (IC_{50} = 108 μmol/l). In contrast, a monoacid analog showed negligible activity, likely a result of insufficient contacts with the two basic Lys591 and Arg609 residues, corroborating the findings of Ren *et al.* [23].

In addition to traditional pTyr mimetics, such as difluoromethylphosphonates, Ge *et al.* [32] designed a novel pTyr unnatural amino acid, wherein the polar phosphate group was replaced by an isoxazole carboxylic acid moiety. In a proof-of-concept study, the Stat3-SH2 domain-binding tripeptide, ISS610 (4-cyanophenyl-pTyr-Leu, Fig. 4-**8**) [33], was modified to replace the pTyr residue with the rationally designed isoxazole amino acid. In a comparative in-vitro study, the isoxazole analog **9** (Fig. 4) was shown to retain moderate inhibitory activity against Stat3's SH2 domain (IC_{50} = 144 μmol/l, as assessed by FP assay) when compared with ISS610. Encouragingly, when T47D cancer cells were treated with both ISS610 and **9** (250 μmol/l) and assessed for inhibition of cell proliferation, **9** was

Fig. 3

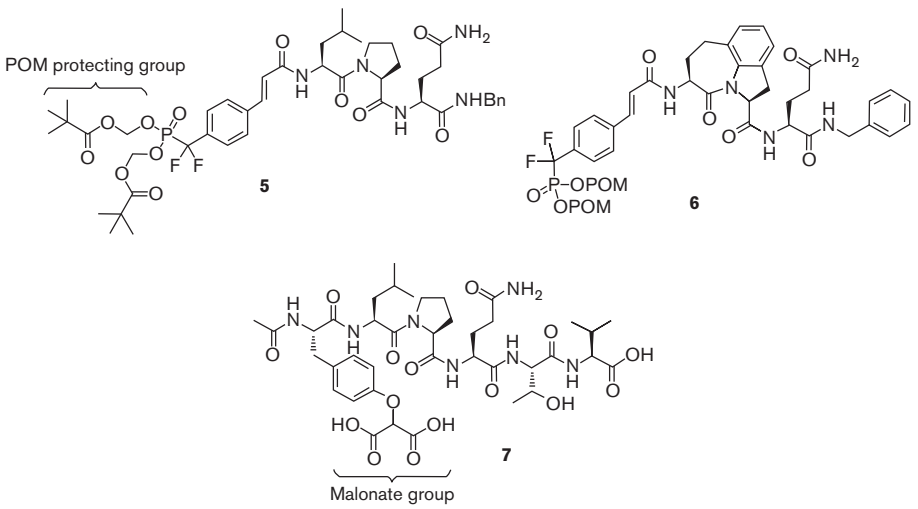

Chemical structures of peptidomimetics **5–7**.

Fig. 4

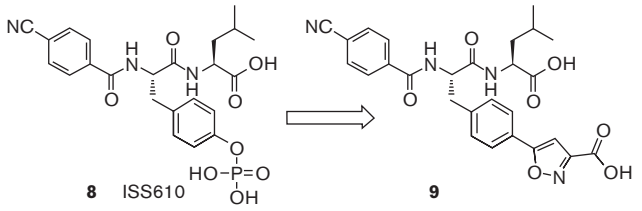

Chemical structures of Stat3 peptidomimetic inhibitor **8** and nonphosphorylated isoxazole analog **9**.

shown to exhibit more potent cellular efficacy, likely a result of improved physiological properties including cell permeability and hydrolytic stability.

Based on the truncated native Stat3 binding sequence, Ac-pYLKTKF-NH_2 (**10**) (IC_{50} = 25.9 μmol/l), Chen *et al.* [34] designed and synthesized a series macrocyclic peptidomimetics using 'click' chemistry. In-silico docking of the peptide to Stat3 showed that the two proximal lysine residues were solvent exposed and did not contribute to binding. The researchers reasoned that these side chains could be cyclized to afford a conformationally constrained peptidomimetic with increased potency and resistance to protease degradation. Thus, the lysine residues in the pY + 2 and pY + 4 positions were replaced with an alkyl azide and alkyne group, respectively, and cyclized under standard click chemistry conditions to furnish **11** (Fig. 5). Using a FP assay, the K_i was determined to be 7.3 μmol/l, an approximate three-fold increase in potency over lead peptide **10**.

Encouraged by their initial successes with the cognate Stat3 binding sequence, Gomez *et al.* [35] extended the rigidification approach to include the gp130 sequence. As part of their strategy, the authors incorporated a series of rigidified Freidinger lactams into a C-terminal and N-terminal benzylated analog of **1** (BnNH-pYLPQ-CONHBn) to afford, among others, inhibitor **12** (Fig. 6). Using a competitive FP assay, the binding affinity (K_i) of **12** was determined to be 190 nmol/l as compared with 390 nmol/l for the lead peptide, BnNH-pYLPQ-CONHBn. Inclusion of the seven-membered lactam ring resulted in a two-fold increase in affinity, and successfully reduced the peptidic character of the lead peptide.

More recently, Chen *et al.* [36] synthesized the bicyclic peptidomimetic scaffold **13**, derived from peptide **1**. By fusing the leucine alkyl side chain to the proline ring, the researchers synthesized a more rigidified bicyclic core. However, peptidomimetic **13** exhibited negligible cellular activity even at relatively high concentrations (100 μmol/l) in MDA-MB-231 and MDA-MB-468 breast cancer cells known to harbor activated Stat3 protein. Likely because of poor cell permeability, the researchers elected to increase the hydrophobicity of the peptidomimetic through N-terminal conjugation to a lipid chain to furnish **14** (Fig. 6).

Fig. 5

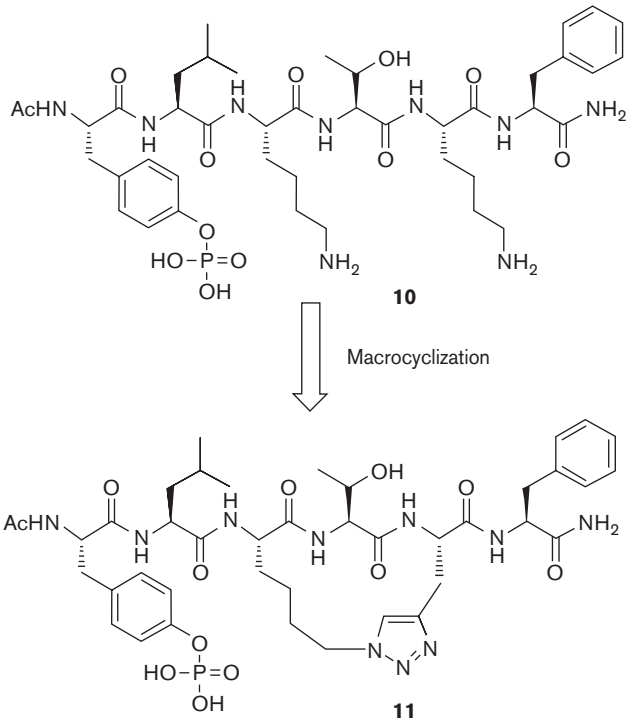

Chemical structures of peptidomimetics **10** and **11**.

Furthermore, the researchers considered the glutamine side chain of **13** to be detrimental to cell permeability, and replaced it with an imidazole group in the **14** analog. Encouragingly, as assessed by FP assay, **14** was calculated to have a K_i of 0.95 μmol/l. Moreover, when evaluated against MDA-MB-231 and MDA-MB-468 cells, **14** exhibited potent cytotoxic effects with IC_{50} values of 11.2 and 3.6 μmol/l, respectively. In addition, **14** was found to significantly reduce levels of phosphorylated Stat3 and decrease the levels of Stat3 transcriptional targets (Bcl-x_L and cyclin D1) at 5–10 μmol/l inhibitor concentrations. Stat3 phosphorylation requires recruitment to intracellular kinases through the SH2 domain. Thus, the observed abolition of Stat3 phosphorylation, despite extracellular stimulation, indicates that **14** binds the Stat3 SH2 domain and prevents phosphorylation.

Small molecule inhibitors

Peptidomimetic strategies have served to identify novel peptide-inspired inhibitors and to facilitate the design of nonpeptidic small molecules. For example, inspired by the peptidomimetic ISS610 (Fig. 4), Gunning *et al.* [37] rationally designed a novel class of non-peptidic, oxazole and thiazole-based small molecule Stat3 inhibitors. Identified through the synthesis of a focused library of inhibitors, oxazole S3I-M2001 (**15**, Fig. 7) and PGB2-105 (**16**) showed promising in-vitro activity, effectively disrupting Stat3–Stat3 dimers, as assessed by EMSA

Fig. 6

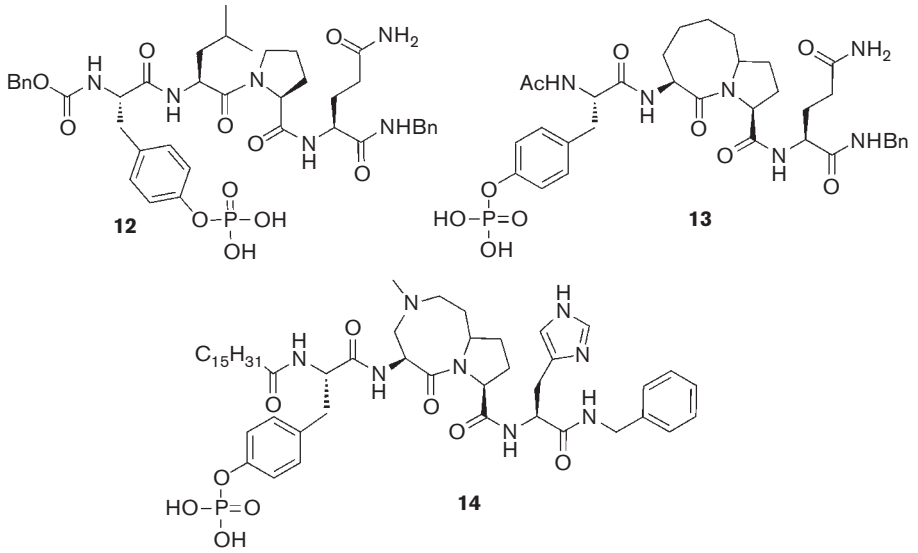

Chemical structures of structurally rigidified peptidomimetics **12–14**.

assay. The researchers identified a trisubstituted heterocyclic core as being a good mimetic of ISS610, and suitably projected binding functionality to access the three sub-pockets of the SH2 domain. Both **15** and **16** incorporated a trisubstituted oxazole core substituted at C5 with a phosphotyrosyl appendage and both C2 (**15**, C2 = phenyl; **16**, C2 = naphthyl) and C4 (**15**, C4 = cyclohexylbenzyl; **16**, C4 = hexyl) positions were furnished with hydrophobic substituents. Lead inhibitors were assessed for the biochemical and biological activities in MDA-MB-468 breast cancer cells [38]. The hydrophobic components of both **15** and **16** occupied the subdomains predominantly composed of nonpolar residues including Phe716, Met660 and Pro715. As assessed by an in-vitro DNA-binding electrophoretic mobility shift (EMSA) assay, **15** displayed an $IC_{50} = 78\,\mu mol/l$ *cf.* **15**, $IC_{50} = 33\,\mu mol/l$. In addition, in-vitro treatment of 'normal' NIH3T3 fibroblasts versus Stat3-containing NIH3T3/vSrc-transformed cells with **15** and **16** resulted in an approximately 10-fold specificity for NIH3T3/vSrc fibroblasts ($IC_{50} = 120\,\mu mol/l$). The researchers speculated that the more hydrophilic and 'drug-like' properties of the oxazole inhibitors facilitated cell permeability. To evaluate the in-vivo potency of **15**, Siddiquee *et al.* showed that **15** prevented Stat3-dependent malignant transformation, survival, migration, and invasion of mouse and human cancer cells that harbor constitutively activated Stat3. In particular, **15** inhibited the growth of MDA-MB-468 human breast cancer xenographs.

In a separate investigation, Siddiquee *et al.* [39] identified a salicylic acid containing small molecule, S3I-201 (**17**, Fig. 7), through in-silico virtual screening of a National

Fig. 7

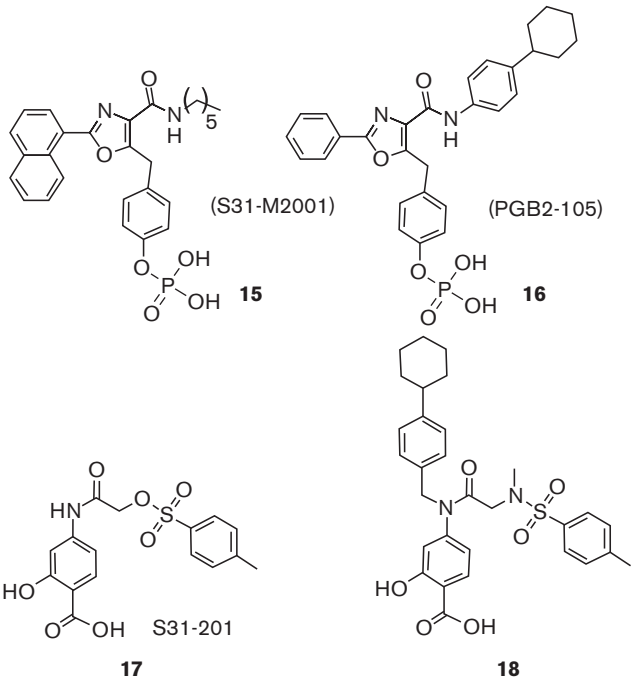

Chemical structures of small molecule inhibitors **15–18**.

Cancer Institute chemical library. S3I-201 was shown to inhibit Stat3 function in cells ($IC_{50} = 86\,\mu mol/l$, as assessed by EMSA analysis of nuclear extracts) and showed promising in-vivo activity in breast tumor xenografts (MDA-MB-231) in mice models. The salicylic group was shown to be a potent phosphate mimetic, consistently

docking within the pTyr-binding site. From a drug discovery perspective, the retention of binding activity despite the lack of a polar pTyr moiety was particularly promising. However, S3I-201 suffered from several drawbacks, including (i) the presence of an electrophilic tosyl leaving group, rendering it highly susceptible to alkylation and (ii) poor physical occupation of Stat3's three subdomains. As visualized by genetically optimized ligand docking, S3I-201 failed to occupy the binding site composed of Trp623, Val637, Ile569, and Phe716.

In a subsequent structure–activity relationship (SAR) study of the S3I-201 structure, Fletcher *et al.* [40] showed *in silico* that N-alkylation of the S3I-201 secondary amide with a range of hydrophobic substituents afforded better occupation of the SH2 domain. To better determine the structure–activity relationships, Fletcher *et al.* replaced the problematic oxygen atom of the tosylate with an *N*-methyl group to yield a nonlabile tosylamide. Thus, the authors synthesized a small series of N-alkylated S3I-201 analogs, culminating in the identification of SF-1-066 (**18**, Fig. 7), a cyclohexylbenzyl containing inhibitor. It was shown that SF-1-066 potently disrupted Stat3-Stat3:DNA binding ($IC_{50} = 35$ μmol/l), with an approximate three-fold increase in activity. The EMSA data were corroborated with FP assay conformation of SH2 binding ($K_i = 29.8$ μmol/l). In addition, subsequent specificity experiments conducted by Zhang *et al.* [41] in epidermal growth factor receptor-stimulated NIH3T3 cells containing activated Stat1, Stat3, and Stat5 proteins, showed impressive Stat3 specificity by **18**. Moreover, in a water-soluble tetrazolium salt-1 cytotoxicity assay, **18** showed potent activity in Stat3-containing cell lines MDA-MB-468 [42], DU145 [43], and OCI-AML2 [44], with IC_{50} values of 17, 37, and 36 μmol/l, respectively. In comparison, S3I-201 required 100 μmol/l concentrations to achieve similar results [41]. Notably, **18** did not inhibit HL60 or NIH3T3 cell viability, both of which lack activated Stat3.

Fuh *et al.* [45] have developed a potent anthracene-based, small molecule inhibitor of Stat3 function, LLL-3 (**19**) (Fig. 8). LLL-3, a structural analog of the earlier identified STA-21 [46], was rationally developed from STA-21 through a structure-based design strategy aided by in-silico docking with the Stat3 SH2 domain. The researchers reasoned that the lower molecular weight of **19** (**19**, MWt. = 266 *cf.* STA-21, MWt. = 306) would enhance the cell permeability and be a more drug-like Stat3 inhibitor. LLL-3 was tested in Stat3-containing human glioblastoma cells at 10–40 μmol/l concentrations and shown to significantly decrease cell viability (< 25%). Encouragingly, at 30 μmol/l, **19** decreased the cell viability to less than 10% in U87, U251, and U373 glioblastoma cells. In addition, intracranial U87 glioblastoma tumors generated in nude mice treated with **19** exhibited significantly smaller and less hyperintense tumors than those of the control models.

Fig. 8

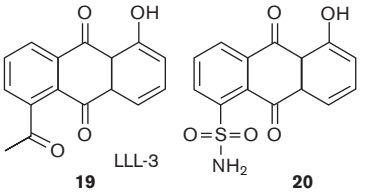

Chemical structures of small molecules **19** and **20**.

In a separate study involving **19**, Mencalha *et al.* [47] investigated the effects of **19** in K562 leukemia cells, containing constitutively active Stat3 as a result of aberrant BCR-ABL tyrosine kinase activity. K562 cells were significantly inhibited after the treatment with 40 μmol/l of **19** in a dose-dependent and time-dependent manner at 24 h ($IC_{50} = 37$ μmol/l) and 48 h ($IC_{50} = 6.3$ μmol/l). For comparison, Mencalha *et al.* [47] evaluated **19** in Stat3-containing DU145 prostate cancer cells, and non-Stat3-containing MCF-7 breast cancer cells and showed impressive specificity for DU145 cells (DU145, $IC_{50} = 11.3$ μmol/l *cf.* MCF-7, $IC_{50} = 150$ μmol/l). For the effective treatment of K562 leukemia cells, Abdelhay *et al.* logically conducted a combination therapy with **19** and imatinib mesylate (IM), an inhibitor of BCR-ABL's tyrosine kinase activity. Cotreatment of K562 cells with **19** (40 μmol/l) and IM (1 μmol/l) resulted in an increase of nonviable K562 cells by 21% after 24 h compared with IM treatment alone. As a control, the researchers tested the combination therapy in BCR-ABL-positive and negative cells, MBA and Mo7e, respectively. In the BCR-ABL-positive MBA cell lines, treatment with 40 μmol/l **19** and 1 μmol/l IM resulted in an enhanced decrease in the cell proliferation (18% after 24 h) compared with IM treatment alone. Furthermore, in Mo7e-negative cells, the combination strategy had negligible effect on cell viability. To assess for cell viability, K562 cells were treated in combination with **19** or with IM alone and measured with using a water-soluble tetrazolium salt-1 viability assay. When treated in combination, there was an approximately two-fold increase in observed apoptosis (47.5% *cf.* 28.5%) after a 24 h period. These findings suggest that **19** is a promising inhibitor of Stat3 function and a promising combination partner of IM for the treatment of K562 leukemia cells.

In a subsequent study, Lin *et al.* [48] identified LLL-12 (**20**, Fig. 8), a structurally analogous compound to **19**, whereby the acetyl group present in **19** was replaced with a sulfonamide. In-silico docking of **20** with the SH2 domain showed greater binding interactions between the sulfonamide group and the protein surface. As with **19**, Lin *et al.* confirmed Stat3–Stat3 dimer disruption by **20** through EMSA analysis of DNA binding. Treatment of Stat3-dependent breast cancer cells (MDA-MB-231 and

SK-BR-3), pancreatic cancer cells (HPAC and PANC-1), and glioblastma cells (U87 and U373) with only 5 μmol/l of **20** was sufficient to downregulate Stat3 phosphorylation protein levels and induce apoptosis. Examination of Stat3 downstream transcriptional targets showed that treatment with **20** suppressed cyclin D1, survivin, and Bcl-2 at both the protein and messenger RNA levels. Given the importance of developing and identifying Stat3 inhibitors with potent whole-cell activity, the presented data were highly encouraging. To further probe the efficacy of this promising therapeutic, Lin *et al.* conducted in-vivo antitumor studies in breast (MDA-MB-231) and glioblastoma (U87) xenograft models. Excitingly, both breast and glioblastoma tumors were significantly suppressed by the treatment with **20** when compared with dimethyl sulfoxide-treated controls. Compound **20** shows significant potential as a Stat3-SH2 domain inhibitor.

Flavonoids have been used as herbal remedies for centuries and are renowned for their antioxidant, anti-inflammatory, antiviral, and antitumor activities. In particular, flavopiridol (**21**, Fig. 9), a synthetic derivative of flavone, was the first reported cyclin-dependent kinase inhibitor to enter clinical trials [49]. A recent study by Lee *et al.* [50] has shown that flavopiridol attenuated Stat3-directed transcription (as assessed by a Stat3-dependent luciferase reporter assay), disrupted dimeric Stat3–Stat3:DNA interaction (EMSA DNA binding assay), and downregulated the expression of Stat3 mediated antiapoptotic signals. Specifically, flavopiridol was shown to decrease the expression levels of Stat3-regulated transcriptional targets, Mcl-1, cyclin D1, and cyclin A. The reserachers also reported a synergistic combination strategy involving flavopiridol and the JAK kinase inhibitor, AG490. The combination of flavopiridol and AG490 produced cytotoxic synergy, yielding combination indices in the range of 0.2–0.5, in which indices less than 1 are indicative of synergy.

Resveratrol (**22**, Fig. 9) (*trans*-3,5,4′-trihydroxystilbene) has been found to inhibit levels of phosphorylated Stat3 activity and exhibited potent antiproliferative properties in human cancers such as breast cancer [51], oral cancer [52,53], prostate cancer [54,55], and leukemia [56]. A resveratrol analog, DMU-212 (**23**, Fig. 9) (3,4,5,4′-tetra-methoxystilbene) was shown by Sale *et al.* [57] to display enhanced antiproliferative activity in colon cancer. In addition, both **22** and **23** elicited reductions in the levels of phosphorylated Stat3 protein in MDA-MB-435 and MCF-7 breast cancer cell lines and was shown to downregulate Stat3-induced genes, including cyclin D1 and Bcl-x_L. After continuous exposure to various concentrations of **22** and **23**, MDA-MB-435 and MCF-7 breast cancer cells showed a dose-dependent decrease in cell viability relative to negative control cultures. For MDA-MB-435 cells, **23** was more potent than **22**, affording an IC_{50} value six times lower than that of resveratrol after 48 h of treatment (9.9 vs. 69.3 μmol/l). However, for MCF-7 cells, which are less sensitive to these treatments in comparison with MDA-MB-435 cells, DMU-212 was only slightly more active than **22** at concentrations of 50 μmol/l or lower.

High-throughput screening

In-silico screening

STA-21 (Fig. 10, **24**) was discovered by Song *et al.* [46] as a novel Stat3-SH2 targeting inhibitor through a virtual screen of 429 000 compounds from the National Cancer Institute, Merck Index, Sigma-Aldrich, and Ryan Scientific catalogs. Song *et al.* identified **24** after screening the top 100 in-silico candidates with a Stat3-dependent luciferase reporter. Furthermore, **24** showed potent disruption of Stat3 dimerization and DNA binding, inhibited Stat3 nuclear translocation and downregulated Stat3 target genes such as Bcl-X_L and cyclin D1. In addition, **24** reduced the growth and survival of Stat3-dependent breast carcinoma cells lines, MDA-MB-231, MDA-MB-435s, and MDA-MB-468 at micromolar concentrations. Encouragingly, **24** had a minimal inhibitory effect against Stat3-independent MCF7 and MDA-MB-453 breast carcinoma cells and human skin fibroblasts. At 20 μmol/l, **24** abolished Stat3 dimerization in MDA-MB-435s cells after 24 h. Wary of targeting upstream effectors, the authors showed that **24** did not inhibit the phosphorylation of JAK2, Src, and EGFR. Docking studies showed that **24** makes significant binding contacts and interacts with key residues in the SH2 domain such as Arg-595, Arg-609, and Ile-634. The researchers cited the presence

Fig. 9

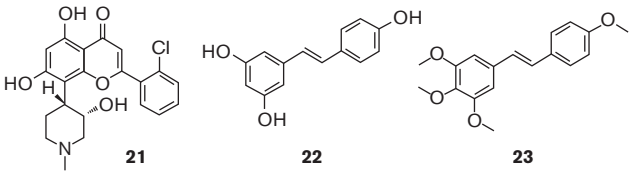

Chemical structures of small molecules **21**, **22** and **23**.

Fig. 10

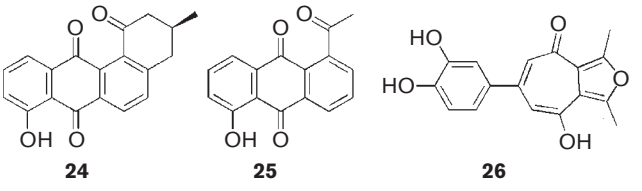

Chemical structures of STA-21 (**24**), anthriquinone (**25**), and catechol **26**.

of the synthetically problematic benzo[*a*]anthracene-1,7,12-trione core as a drawback to rapidly generate an effective SAR.

In an effort to reduce the synthetic challenge of generating a SAR library, Bhasin *et al.* [58] simplified the sophisticated benzo[*a*]anthracene-1,7,12-trione moiety of **24** to produce a small library of structurally similar anthraquinone analogs. Docking analysis of the analogs through Autodock (v 4.0) showed that compound **25** (Fig. 10) most notably resembled the docking patterns of **24**. A physical sample of this compound in calorimetric membrane translocation sequence assay exhibited comparable low-micromolar, whole-cell activity in prostate cancer cell lines DU145, PC3, and LNCaP and the breast cancer cell line MCF-7.

In another study, Hao *et al.* [59] conducted an in-silico screening of 100,000 and more compounds from the Wyeth's proprietary small-molecule library to test for their binding to the SH2 domain of Stat3. The top 1000 candidates were evaluated *in vitro* by ELISA for their ability to disrupt dimeric Stat3:DNA complex formation. Researchers reported the presence of a common catechol moiety in a group of compounds that exhibited potency in binding to the SH2 domain. Further screening of the catechol-containing compounds identified compound **26** with an IC_{50} value of 106 µmol/l. Docking studies using GLIDE showed that the catechol moiety docked into the pTyr-binding pocket and made hydrogen bonds with the conserved pTyr-binding residues, Arg609 and Glu612. The researchers suggest that the catechol moiety may be a pTyr bioisostere and can be used to develop cell permeable Stat3 inhibitors.

In-vitro screening

Cryptotanshinone (**27**, Fig. 11) is an archetypal naturally occurring substance that is a major constituent of the tanshinone family. Tanshinones are isolated from the medicinal herb, *Salvia miltiorrhiza* (Danshen) that have been widely used in Chinese traditional medicine as an antioxidative and anti-inflammatory agent. A recent study by Shin *et al.* [60] reported the first evidence of its antiproliferative activity. In this study natural compounds were screened for their ability to inhibit Stat3 activity utilizing a dual luciferase assay. The most potent compound, **27**, suppressed Stat3 signaling in various cancer cell lines and elicited negligible inhibition of upstream Stat3 effectors. Prostate cancer cell line DU145 was most sensitive to **27** (GI_{50} = 7 µmol/l). Further experiments showed that **27** induced decreases in the expression of Stat3-downstream target proteins such as survivin, cyclin D1, and Bcl-xL after 24 h. Other prostate cancer cell lines, PC3 and LNCap, as well as breast cancer cell lines, MDA-MB406, MDA-MB-231 and MCF-10A, which harbor lower levels of Stat3 activity, showed minimal growth inhibition in response to treatment with **27**.

Fig. 11

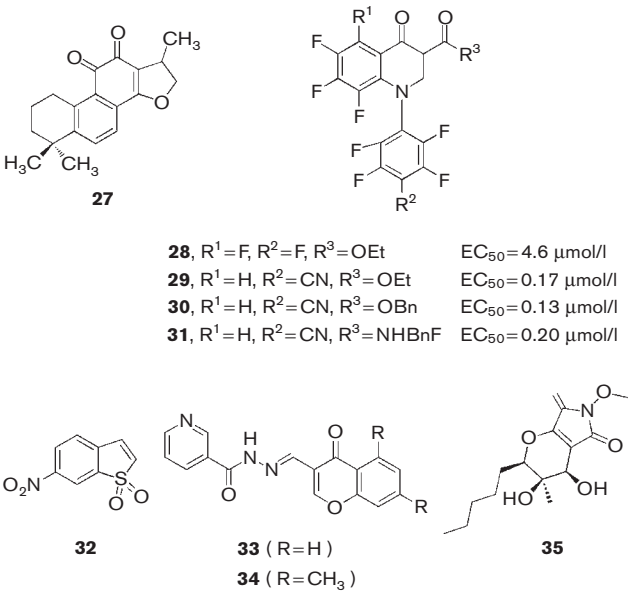

Chemical structures of small molecules **27–35**.

To study the binding mechanism of cryptotanshinone, proteins upstream of Stat3, such as the JAK protein family and Src, were investigated. The phosphorylation of the JAK family was suppressed after treatment with 7 µmol/l **27** (4 h). However, Stat3 phosphorylation was inhibited within only 30 min of treatment, indicating that inhibition of Stat3-Tyr705 phosphorylation is a JAK2 independent event. Further studies were conducted to investigate the binding selectivity of **27** to Stat3 in DU145 cells. Experiments showed the colocalization of cryptotanshinone with Stat3 in the cytoplasm and resulted in the suppression of Stat3 dimerization. This result was in agreement with the author's computational modeling studies that indicated direct cryptotanshinone-SH2 domain binding [60].

Using a high-throughput Apo-ONE Homogenous Caspase 3/7 assay in U266 cells, Xu *et al.* [61] reported the discovery of quinoline derivatives as potent Stat3 inhibitors. Western blot analysis of inhibitor-treated U266 cells identified compound **28** as an effective inhibitor of Stat3-Tyr705 phosphorylation and its upstream regulators. Structural exploration of **28** led to the identification of **29**, which more potently inhibited Stat3-Tyr705 phosphorylation (EC_{50} = 170 nmol/l). Using an in-vitro kinase assay, the researchers showed that **29** inhibited cytokine-induced activation of JAK1, JAK2, and Tyk2 while not affecting the enzymatic activity of the JAK proteins. In addition to **29**, Xu *et al.* [61] showed that analogs **30** and **31** (Fig. 11) downregulated the expression of Stat3 target genes. Despite the exact mode of action remaining unclear, the data suggest that these quinoline derivatives are potent and selective inhibitors of the JAK/STAT pathway.

In another study, Schust *et al.* [62] conducted a high-throughput screen of a chemical library (17 000 compounds) using a competitive FP assay designed by the same group. The researchers identified Stattic (Fig. 11, **32**), a small molecule that, on further investigation, was shown to selectively inhibit Stat3 activation, dimerization, and nuclear translocation. Moreover, Stattic was shown to be isoform-selective for Stat3, and specific for Stat3 over other SH2-containing proteins. Moreover, at 10 μmol/l, Stattic reduced Stat3 phosphorylation and induced apoptosis in Stat3-containing breast cancer cell lines, MDA-MB-231 and MDA-MB-435s. In attempts to elucidate the mode of action, the researchers found that the potency of **32** was temperature-dependent, displaying only weak activity at 22°C, but more highly potent at a physiological temperature of 37°C (IC_{50} = 5 μmol/l). Furthermore, subsequent SAR studies showed that saturation of the vinylic sulfone component resulted in the loss of activity. Thus, taken in conjunction, the researchers suggested that Stattic may function as a Michael-acceptor alkylating agent, and inhibit Stat3 by covalently coupling to the Stat3 SH2 domain [63].

Further to this study, Muller *et al.* [64] later reported the discovery of several inhibitors of the Stat5β and Stat3 SH2 domains. Most notably, using a Stat5 high-throughput FP assay [65,66], a series of chromone-derived acyl hydrazone compounds that exhibited micromol per liter affinities for the SH2 domain of Stat5β were reported. Most notably, compound **33** (Fig. 11) bound the Stat5β SH2 domain with an IC_{50} of 47 μmol/l. The researchers also reported a new chromone-based Stat3 inhibitor **34**, which displayed preferential inhibition of Stat3 (IC_{50} = 107 μmol/l) over the Stat5β isoform (IC_{50} = 217 μmol/l), as assessed by FP assay. Removing the chromone group resulted in a loss of activity, possibly identifying the chromone motif as a STAT pharmacophore. Maloney *et al.* [67] identified the bicyclic natural product, phaeosphaeride A (Fig. 11, **35**) as a Stat3 inhibitor through the screening of a predominantly natural product library consisting of 10 000 compounds in an ELISA-based screen. The researchers reported **35** to be a moderate Stat3 inhibitor (IC_{50} = 0.62 mmol/l). Compound **35** showed promising inhibition of Stat3-dependent signaling pathways compared with its diastereomer, phaeosphaeride B, which displayed no activity. Moreover, **35** showed preference for Stat3 over both Stat5 and Stat1 isoforms. Interestingly, when evaluated *in vivo*, compound **35** showed potency both in a Stat3-dependent U266 multiple myeloma cell line (IC_{50} = 6.7 μmol/l) and in a Stat3-independent K562 cell line, in which it exhibited similarly low micromolar activity. This result suggests that **35** may have additional off-target effects in whole cells [68].

Metal-based Stat3 inhibitors

Platinum complexes, such as cisplatin (Fig. 12), have been widely used in chemotherapy to cross-link sub-units of DNA and impair cellular function. For example, cisplatin was reported to downregulate the JAK/STATs pathway through DNA alkylation. However, Turkson *et al.* [69] showed that platinum complexes could be used in a nontraditional role, and were shown to directly suppress Stat3 function. In particular, a variety of platinum(IV) complexes displayed low micromol per liter inhibition of Stat3–Stat3 dimerization. Encouragingly, CPA-7 **37** (Fig. 12) exhibited STAT isoform selectivity, preferentially inhibiting Stat3 over both Stat1 and Stat5 (Stat3, IC_{50} = 1.5 μmol/l

Fig. 12

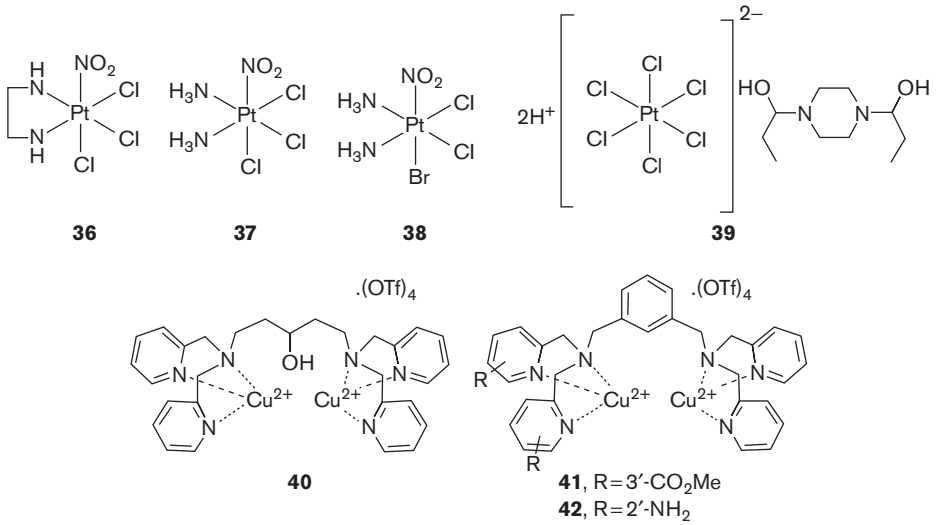

Chemical structures of metal complexes **36–42**.

cf. Stat1, $IC_{50} = 4.0\,\mu mol/l$). Furthermore, Turkson *et al.* [69] showed that **37** suppressed colon CT26 tumors in mouse models. Subsequent analysis of tumor samples showed decreased Stat3 activity.

In a subsequent related study, Turkson *et al.* [70] discovered a platinum-based agent that selectively attenuated Stat3 signaling in human and mouse tumor cells [63]. Inhibitor IS3295 (**39**) was reported to selectively disrupt Stat3 ($IC_{50} = 1.4\,\mu mol/l$), while displaying moderately weaker affinity for the Stat1 isoform ($IC_{50} = 4.1\,\mu mol/l$). Furthermore, **39** potently suppressed the expression of Stat3-regulated genes such as cyclin D1 and Bcl-x_L, suggesting that it elicits antiproliferative activity by blocking cell growth and antiapoptotic signaling, and thus promoting apoptosis.

Most recently, Drewry *et al.* reported the design and synthesis of a novel family of $Cu(II)_2$-bis-dipicolylamine coordination complexes that display potent anti-Stat3 activity (Fig. 12, **40–42**). In contrast to most Stat3 inhibitors, which target the SH2 domain, Drewry *et al.*, instead, targeted the cognate phosphopeptide binding sequence of Stat3. Using the Lewis acidic metal complexes, the researchers aimed to bind the Lewis basic pTyr group of the phosphopeptide and disrupt the phosphorylated Stat3 binding partner. Using isothermal titration calorimetry, Drewry *et al.* [71] showed promising binding affinities for truncated Stat3 and gp130 phosphorylated sequences (K_i values approximately 8 to 100 μmol/l). Next, a competitive FP assay was used to assess the metal complex mediated disruption of Stat3 protein–phosphopeptide interactions. Notably, compounds **41** and **42** disrupted the Stat3 protein–phosphopeptide complex with K_i values of 15 and 38 μmol/l, respectively. Moreover, in-vitro EMSA analysis of Stat3–Stat3:DNA disruption showed therapeutic efficacy, with **41** and **42** displaying similar IC_{50} values of 74 and 41 μmol/l, respectively. Furthermore, the researchers reported that select inhibitors displayed a three-fold preference for Stat3 over its isoform Stat1 (Stat3, $IC_{50} = 61\,\mu mol/l$ *cf.* Stat1, $IC_{50} = 176\,\mu mol/l$). Further investigation showed that the unchelated $Cu(II)_2$-bis-dipicolylamine ligands had negligible effect on Stat3–Stat3:DNA ternary complex. Taken in conjunction, the researchers suggested that the Lewis acidic metal complexes inhibit Stat3 by mimicking the pTyr-binding function of the SH2 domain. In addition, **41** exhibited highly promising biological effects in the Stat3-dependent DU145, MDA 468, and OCI-AML2 cancer cells at very low micromolar concentrations (5–10 μmol/l). Furthermore, the cell viability studies at similar concentrations in healthy cells (NIH3T3) showed minimal cytotoxicity. This approach to disrupting Stat3 dimerization represents an exciting and promising class of therapeutics.

Discussion

Stat3's critical dysregulatory and oncogenic role in many human cancers makes it a highly attractive target for novel molecular therapeutics. However, protein–protein interactions remain a daunting target for disruption by small molecules because of their often large interfacial areas and noncontiguous contact points. The vast majority of the present drug discovery effort is focused on phosphopeptide mimetics, which have major pharmacokinetic and pharmacodynamic drawbacks because of polarity and lability, as was reported in many early peptidic strategies. It is important to note that, despite these significant hurdles, current drug discovery approaches targeting the SH2 domain have uncovered several potent Stat3 inhibitors (nmol/l) with in-vivo efficacy. In the past decade, medicinal chemists have made substantial advancements in inhibitor potency. Although a Stat3-targeting drug has yet to reach the clinic, the recent flurry of impressive work highlighted in this review, particularly over the last 2 years, gives a strong indication that potent and clinically viable Stat3 homodimer and heterodimer inhibitors are possible and getting closer. Despite the obvious high-risk drawbacks of targeting oncogenic protein–protein interactions, disrupting Stat3 protein dimerization is emerging as a suitable and executable therapeutic target.

References

1 Buettner R, Mora LB, Jove R. Activated STAT signaling in human tumors provides novel molecular targets for therapeutic intervention. *Clin Cancer Res* 2002; **8**:945–954.

2 Bowman T, Garcia R, Turkson J, Jove R. STATS in oncogenesis. *Oncogene* 2000; **19**:2474–2488.

3 Darnell JE Jr. STATs in gene regulation. *Science* 1997; **277**:1630–1635.

4 Darnell JE Jr, Kerr IM, Stark GR. Jak-STAT pathways and transcriptional activation in response to IFNs and other extracellular signaling proteins. *Science* 1994; **264**:1415–1421.

5 Stark GR, Kerr IM, Williams BR, Silverman RH, Schreiber RD. How cells respond to interferons. *Annu Rev Biochem* 1998; **67**:227–264.

6 Ma J, Cao X. Regulation of STAT3 nuclear import by importin α5 and importin α7 via two different functional sequence elements. *Cell Signal* 2006; **18**:1117–1126.

7 Zhang T, Kee WH, Seow KT, Fung W, Cao X. The coiled-coil domain of STAT3 is essential for its SH2 domain-mediated receptor binding and subsequent activation induced by epidermal growth factor and interleukin-6. *Mol Cell Biol* 2000; **20**:7132–7139.

8 Becker S, Groner B, Müller C. Three-dimensional structure of the STAT3β homodimer bound to DNA. *Nature* 1998; **394**:145–151.

9 Yang E, Wen Z, Haspel RL, Zhang JJ, Darnell JE Jr. The linker domain of STAT1 is required for gamma interferon-driven transcription. *Mol Cell Biol* 1999; **19**:5106–5112.

10 Catlett-Falcone R, Dalton WS, Jove R. STAT proteins as novel targets for cancer therapy. *Curr Opin Oncol* 1999; **11**:490–496.

11 Catlett-Falcone R, Landowski TH, Oshiro MM, Turkson J, Levitzki A, Savino R, *et al.* Constitutive activation of STAT3 signaling confers resistance to apoptosis in human U266 myeloma cells. *Immunity* 1999; **10**:105–115.

12 Sinibaldi D, Wharton W, Turkson J, Bowman T, Peters G, Pledger WJ, Jove R. Induction of p21WAF1/CIP1 and cyclin D1 expression by the Src oncoprotein in mouse fibroblasts: role of activated STAT3 signaling. *Oncogene* 2000; **19**:5419–5427.

13 Kujawski M, Kortylewski M, Lee H, Herrmann A, Kay H, Yu H. Stat3 mediates myeloid cell-dependent tumor angiogenesis in mice. *J Clin Invest* 2008; **118**:3367–3377.

14 Duan Z, Foster R, Bell DA, Mahoney J, Wolak K, Vaidya A, *et al.* Signal transducers and activators of transcription 3 pathway activation in drug-resistant ovarian cancer. *Clin Cancer Res* 2006; **12**:5055–5063.

15 Burke WM, Jin X, Lin H, Huang M, Liu R, Reynolds RK, Lin J. Inhibition of constitutively active STAT3 suppresses growth of human ovarian and breast cancer cells. *Oncogene* 2001; **20**:7925–7934.

16 Abdulghani J, Gu L, Dagvadorj A, Lutz J, Leiby B, Bonuccelli G, *et al.* STAT3 promotes metastatic progression of prostate cancer. *Am J Pathol* 2008; **172**:1717–1728.

17 Holtick U, Vockerodt M, Pinkert D, Schoof N, Stürzenhofecker B, Kussebi N, *et al.* STAT3 is essential for Hodgkin lymphoma cell proliferation and is a target of tyrphostin AG17 which confers sensitization for apoptosis. *Leukemia* 2005; **19**:936–944.

18 Zhang Q, Raghunath PN, Xue L, Majewski M, Carpentieri DF, Odum N, *et al.* Multilevel dysregulation of STAT3 activation in anaplastic lymphoma kinase-positive T/Null-cell lymphoma. *J Immunol* 2002; **168**:466–474.

19 Leeman RJ, Lui WW, Grandis JR. STAT3 as a therapeutic target in head and neck cancer. *Expert Opin Biol Ther* 2006; **6**:231–241.

20 Kotenko SV, Pestka S. Jak-Stat signal transduction pathway through the eyes of cytokine class II receptor complexes. *Oncogene* 2000; **19**:2557–2565.

21 Bromberg JF. Activation of STAT proteins and growth control. *Bioessays* 2001; **23**:161–169.

22 Turkson J, Ryan D, Kim JS, Zhang Y, Chen Z, Haura E, *et al.* Phosphotyrosyl peptides block Stat3-mediated DNA binding activity, gene regulation, and cell transformation. *J Biol Chem* 2001; **276**:45443–45455.

23 Ren Z, Cabell LA, Schaefer TS, McMurray JS. Identification of a high-affinity phosphopeptide inhibitor of Stat3. *Bioorg Med Chem Lett* 2003; **13**:633–636.

24 Diurlat J, Liu W-Q, Sancier F, Edmonds T, Pamonsinlapatham P, Cruzalegui F, *et al.* A novel non-phosphorylated potential antitumoral peptide inhibits STAT3 biological activity. *Biochimie* 2009; **91**:996–1002.

25 Coleman DR IV, Ren Z, Mandal PK, Cameron AR, Dyer GA, Muranjan S, *et al.* Investigation of the binding determinants of phosphopeptides targeted to the Src homology 2 domain of the signal transducer and activator of transcription 3. Development of a high-affinity peptide inhibitor. *J Med Chem* 2005; **48**:6661–6670.

26 Mandal PK, Ren Z, Chen X, Xiong C, McMurry JS. Conformationally constrained peptidomimetic inhibitors of signal transducer and activator of transcription 3: evaluation and molecular modeling. *J Med Chem* 2009; **52**:2429–2442.

27 Mandal PK, Heard PA, Ren Z, Chen X, McMurray JS. Solid-phase synthesis of Stat3 inhibitors incorporating *O*-carbamoylserine and *O*-carbamoylthreonine as glutamine mimics. *Bioorg Med Chem Lett* 2007; **17**:654–656.

28 Mandal PK, Limbrick D, Coleman DR IV, Dyer GA, Ren Z, Birtwistle S. Structure–affinity relationships of glutamine mimics incorporated into phosphopeptides targeted to the SH2 domain of signal transducer and activator of transcription 3. *J Med Chem* 2009; **52**: 2429–2442.

29 McMurray JS. Structural basis for the binding of high affinity phosphopeptides to Stat3. *Biopolymers* 2008; **90**:69–79.

30 Mandal PK, Liao WS-L, McMurray JS. Synthesis of phosphatase-stable, cell-permeable peptidomimetic prodrugs that target the SH2 domain of STAT3. *Org Lett* 2009; **11**:3394–3397.

31 Dourlat J, Valentin B, Liu W-Q, Garbay C. New syntheses of tetrazolylmethylphenylalanine and *O*-malonyltyrosine as pTyr mimetics for the design of STAT3 dimerization inhibitors. *Bioorg Med Chem Lett* 2007; **17**:3943–3946.

32 Ge J, Wu H, Yao SQ. An unnatural amino acid that mimics phosphotyrosine. *Chem Comm* 2010; **46**:2980–2982.

33 Turkson J, Kim JS, Shumin Z, Yuan J, Huang M, Glen M, *et al.* Novel peptidomimetic inhibitors of signal transducer and activator of transcription 3 dimerization and biological activity. *Mol Cancer Ther* 2004; **3**: 261–269.

34 Chen J, Nikolovska-Coleska Z, Yang C-Y, Gomez C, Gao W, Krajewski K, *et al.* Design and synthesis of a new, conformationally constrained, macrocyclic small-molecule inhibitor of STAT3 via 'click chemistry'. *Bioorg Med Chem Lett* 2007; **17**:3939–3942.

35 Gomez C, Bai L, Zhang J, Nikolovska-Coleska Z, Chen J, Yi H, Wang S. Design, synthesis, and evaluation of peptidomimetics containing Freidinger lactams as STAT3 inhibitors. *Bioorg Med Chem Lett.* 2009; **19**:1733–1736.

36 Chen J, Bai L, Bernard D, Nikolovska-Coleska Z, Gomez C, Zhang J, *et al.* Structure-based design and conformationally constrained cell-permeable STAT3 inhibitors. *ACS Med Chem Lett.* 2010; **1**:85–89.

37 Gunning PT, Glenn MP, Siddiquee KAZ, Katt WP, Masson E, Saïd M, *et al.* Targeting protein–protein interactions: suppression of STAT3 dimerization with rationally designed small-molecule, nonpeptidic SH2 domain binders. *Chembiochem* 2008; **9**:2800–2803.

38 Siddiquee KAZ, Gunning PT, Glenn M, Katts WP, Zhang S, Schroeck C, *et al.* An oxazole-based small-molecule Stat3 inhibitor modulates Stat3 stability and processing and induces antitumor cell effects. *ACS Chem Biol* 2007; **2**:787–798.

39 Siddiquee K, Zhang S, Guida WC, Blaskovich MA, Greedy B, Lawrence HR, *et al.* Selective chemical probe inhibitor of STAT3, identified through structure-based virtual screening, induces antitumor activity. *Proc Natl Acad Sci U S A* 2007; **104**:7391–7396.

40 Fletcher S, Singh J, Zhang X, Yue P, Page BD, Sharmeen S, *et al.* Disruption of transcriptionally active STAT3 dimers with non-phosphorylated, salicylic acid-based small molecules: potent *in vitro* and tumor cell activities. *Chembiochem* 2009; **10**:1959–1964.

41 Zhang X, Yue P, Fletcher S, Zhao W, Gunning PT, Turkson J. A novel small-molecule disrupts STAT3 SH2 domain-phosphotyrosine interactions and STAT3-dependent tumor processes. *Biochem Pharmacol* 2010; **79**:1398–1409.

42 Garcia R, Yu C, Hudnall A, Carlett R, Nelson KL, Smithgall T. Constitutive activation of Stat3 in fibroblasts transformed by diverse oncoproteins and in breast carcinoma cells. *Cell Growth Diff* 1997; **8**:1267–1276.

43 Mora LB, Buettner R, Seigne J, Diaz J, Ahmad N, Garcia R, *et al.* Constitutive activation of Stat3 in human prostate tumors and cell lines: direct inhibition of Stat3 signaling induces apoptosis of prostate cancer cells. *Cancer Res* 2002; **62**:6659–6666.

44 Spiekermann K, Biethahn S, Wilde S, Hiddemann W, Alves F. Constitutive activation of Stat transcription factors in acute myelogenous leukemia. *Eur J Haematol* 2001; **67**:63–71.

45 Fuh B, Sobo M, Cen L, Josiah D, Hutzen B, Cizek K, *et al.* LLL-3 inhibits STAT3 activity, suppresses glioblastoma cell growth and prolongs survival in a mouse glioblastoma model. *Br J Cancer* 2009; **100**:106–112.

46 Song H, Wang R, Wang S, Lin J. A low-molecular-weight compound discovered through virtual database screening inhibits STAT3 function in breast cancer cells. *Proc Natl Acad Sci U S A* 2005; **102**:4700–4705.

47 Mencalha AL, Rocher BD, Salles D, Binato R, Abdelhay E. LLL-3, a STAT3 inhibitor, represses BCR-ABL-positive cell proliferation, activates apoptosis and improves the effects of imatinib mesylate. *Cancer Chemother Pharmacol* 2010; **65**:1039–1046.

48 Lin L, Hutzen B, Li P-U, Ball S, Zuo M, DeAngelis S, *et al.* A novel small molecule, LLL12, inhibits STAT3 phosphorylation and activities and exhibits potent growth-suppresive activity in human cancer cells. *Neoplasia* 2010; **12**:39–50.

49 Johnson AJ, Lucas DM, Smith LL. Clinical rebirth of flavopiridol in chronic lymphocytic leukemia (CLL): utilizing *in vitro* and *in vivo* pharmacodynamic measurements to improve efficacy and interrogate relevant mechanism(s) of action. *Proc Am Assoc Cancer Res* 2005; **46**:374.

50 Lee YK, Isham CR, Kaufman SH, Bible KC. Flavopiridol disrupts STAT3/DNA interactions, attenuates STAT3-directed transcription, and combines with the Jak kinase inhibitor AG490 to achieve cytotoxic synergy. *Mol Cancer Ther* 2006; **5**:138–148.

51 Mgbonyebi OP, Russo J, Russo IH. Antiproliferative effect of synthetic resveratrol on human breast epithelial cells. *Int J Oncol* 1998; **12**:865–869.

52 Elattar TM, Virji AS. Modulating effect of resveratrol and quercetin on oral cancer cell growth and proliferation. *Anticancer Drugs* 1999; **10**:187–193.

53 Elattar TM, Virji AS. The effect of red wine and its components on growth and proliferation of human oral squamous carcinoma cells. *Anticancer Res* 1999; **19**:5407–5414.

54 Hsieh TC, Wu JM. Differential effects on growth, cell cycle arrest, and induction of apoptosis by resveratrol in human prostate cancer cell lines. *Exp Cell Res* 1999; **249**:109–115.

55 Jones SB, DePrimo SE, Whitfield ML, Brooks JD. Resveratrol-induced gene expression profiles in human prostate cancer cells. *Cancer Epidemiol Biomarkers Prev* 2005; **14**:596–604.

56 Clement MV, Hirpara JL, Chawdhury SH, Pervaiz S. Chemopreventive agent resveratrol, a natural product derived from grapes, triggers CD95 signaling-dependent apoptosis in human tumor cells. *Blood* 1998; **92**:996–1002.

57 Sale S, Tunstall RG, Ruparelia KC, Potter GA, Steward WP, Gescher AJ. Comparison of the effects of the chemopreventive agent resveratrol and its synthetic analog trans 3,4,5,4′-tetramethoxystilbene (DMU-212) on adenoma development in the ApcMin+ mouse and cyclooxygenase-2 in human-derived colon cancer cells. *Int J Cancer* 2005; **115**:194–201.

58 Bhasin D, Cisek K, Pandharkar T, Regan N, Li C, Pandit B, *et al.* Design, synthesis, and studies of small molecule STAT3 inhibitors. *Bioorg Med Chem Lett* 2008; **18**:391–395.

59 Hao W, Hu Y, Niu C, Huang X, Chang C-PB, Gibbons J, Xu J. Discovery of the catechol structural moiety as a Stat3 SH2 domain inhibitor by virtual screening. *Bioorg Med Chem Lett* 2008; **18**:4988–4992.
60 Shin DS, Kim HN, Shin KD, Yoon YJ, Kim SJ, Han DC, Kwon BM. Cryptotanshinone inhibits constitutive signal transducer and activator of trascription 3 through blocking the dimerization in DU145 prostate cancer cells. *Cancer Res* 2009; **69**:193–202.
61 Xu J, Cole DC, Chang C-PB, Ayyad R, Asselin M, Hao W, *et al.* Inhibition of the signal transducer and activator of transcription-3 (STAT3) signaling pathway by 4-oxo-1-phenyl-1,4-dihydroquinoline-3-carboxylic acid esters. *J Med Chem* 2008; **51**:4115–4121.
62 Schust J, Berg T. A high-throughput fluorescence polarization assay for signal transducer and activator of transcription 3. *Anal Biochem* 2004; **330**:114–118.
63 Schust J, Sperl B, Hollis A, Mayer TU, Berg T. Stattic: a small-molecule inhibitor of STAT3 activation and dimerization. *Chem Biol* 2006; **13**:1235–1242.
64 Muller J, Sperl B, Reindl W, Kiessling A, Berg T. Discovery of chromone-based inhibitors of the transcription factor STAT5. *Chembiochem* 2008; **9**:723–727.
65 Quelle FW, Wang D, Nosaka T, Thierfelder WE, Stravopodis D, Weinstein Y, Ihle JN. Erythropoietin induces activation of stat5 through association with specific tyrosines on the receptor that are not required for a mitogenic response. *Mol Cell Biol* 1996; **16**:1622–1631.
66 May P, Gerhartz C, Heesel B, Welte T, Doppler W, Graeve L, Horn F, Heinrich PC. Comparative study on the phosphotyrosine motifs of different cytokine receptors involved in STAT5 activation. *FEBS Lett* 1996; **394**:221–226.
67 Maloney KN, Hao W, Xu J, Gibbons J, Hucul J, Roll D, *et al.* Phaeosphaeride A, an inhibitor of STAT3-dependent signaling isolated from an endophytic fungus. *Org Lett* 2006; **8**:4067–4070.
68 Song H, Sondak VK, Barber DL, Reid TJ, Lin K. Modulation of Janus kinase 2 by cisplatin in cancer cells. *Int J Oncol* 2004; **24**:1017–1026.
69 Turkson J, Zhang S, Palmer J, Kay H, Stanko J, Mora LB, *et al.* Inhibition of constitutive signal transducer and activator of transcription 3 activation by novel platinum complexes with potent antitumor activity. *Mol Cancer Ther* 2004; **3**:1533–1542.
70 Turkson J, Zhang S, Mora LB, Burns A, Sebti S, Jove R. A novel platinum compound inhibits constitutive STAT3 signaling and induces cell cycle arrest and apoptosis of malignant cells. *J Biol Chem* 2005; **280**:32979–32988.
71 Drewry JA, Fletcher S, Yue P, Marushchak D, Zhao W, Sharmeen S, *et al.* Coordination complex SH2 domain proteomimetics: an alternative approach to disrupting oncogenic protein–protein interactions. *Chem Commun* 2010; **46**:892–894.